

Harmonic Cyclotron Resonance Scattering Features in the X-Ray Spectrum of 4U 0115+63

Julia Schmid
supervised by Jörn Wilms

October 13, 2008

I analyzed INTEGRAL data of the transient X-ray binary 4U 0115+63 during its most recent outburst (March/April 2008) in a broad energy band (3 – 150 keV). The purpose of this work was to detect cyclotron resonant scattering features (CRSF) and their variations during the observation time. Up to four CRSF could be found. As also seen in former data, I could observe a flux dependent variation of the fundamental line position. Especially the decreasing of the fundamental line energy with the luminosity (from 11.7 keV to 9.19 keV) could be confirmed once more. By the CRSF's position, I could obtain the magnetic field strength $B_{\text{estim}} = 1.31_{-0.03}^{+0.0} \cdot 10^{12}$ G. Furthermore, I found a possible explanation of the “10 keV feature”: analysis of its positions suggests that it is just the emission wing of the fundamental cyclotron line.

By comparing the evaluated flux with BAT count rates, I could estimate its sensitivity to about 41% to 44%.

Contents

| | | |
|----------|---|-----------|
| 1 | Introduction | 3 |
| 2 | Data Analysis | 4 |
| 2.1 | Instruments and Data Reduction | 4 |
| 2.2 | Analysis and Modelling | 5 |
| 3 | Results | 6 |
| 3.1 | Continuum | 6 |
| 3.2 | Flux Variation during the Outburst | 8 |
| 3.3 | Variation of the CRSF with the Flux | 9 |
| 3.4 | Estimation of the Magnetic Field Strength | 11 |
| 3.5 | The “10 keV Feature” | 11 |
| 4 | Summary | 12 |

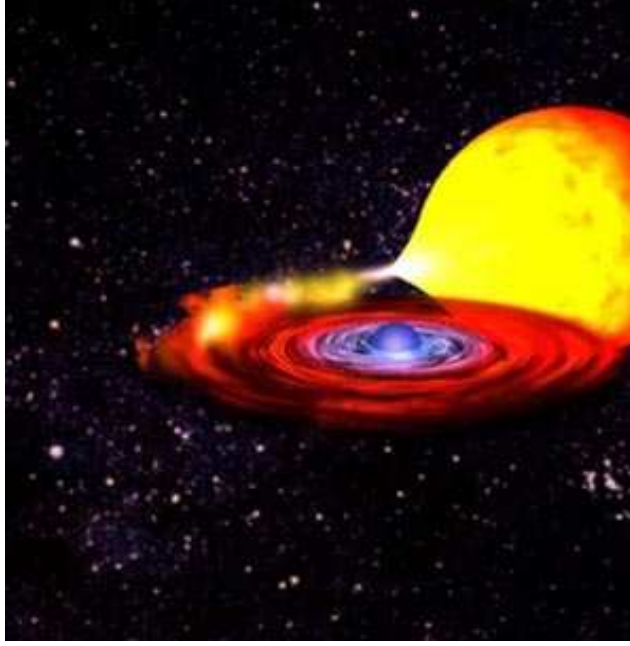


Figure 1: A neutron star X-ray binary. (<http://www.mssl.ucl.ac.uk/~gbr/page6.html>)

1 Introduction

Introductory, I will give a short overview on X-ray binaries and cyclotron lines, mainly following Grämer (2008). 4U 0115+63 is a transient X-ray binary system consisting of a neutron star which is orbiting around a star of type O9e, called V635 Cas. Because of the eccentricity of the orbit the neutron star can at some points enter the gaseous disk around its normal companion. During this time matter falls along the lines of the strong magnetic field onto the poles of the neutron star and most of the released potential energy is emitted as X-rays. Up to now it is not completely understood how the X-ray spectra seen during these outbursts are generated. Models of inverse dynamical and thermal Comptonization could explain the observed form of the continuum (Schönherr et al., 2007), but there are still some features we have to consider.

Electrons in the accreted matter circle around the lines of the magnetic field. But since neutron stars like 4U 0115+63 have some of the strongest magnetic fields in the universe (on the order of 10^{12} Gauss, according to Grämer, 2008), quantum mechanical effects become relevant. As a result, the radii and the allowed energies of the electrons are quantized.

These energy levels (the so-called Landau levels) can be observed as absorption lines (cyclotron resonance scattering features, CRSF) in the spectrum: Photons in the accretion column scatter with the electrons. Because the scattering cross section at the Landau energies is very large compared to the Thomson cross section σ_T (up to $10^6 \sigma_T$ for a magnetic field of $B = 1.7 \cdot 10^{12} G$, as mentioned by Grämer, 2008), photons of the resonant energies cannot leave the accretion column unless their energy has changed by inelastic scattering (see Schönherr et al., 2007).

So far, one would expect one fundamental line and its multiples. But taking relativistic effects and thermal motion of the electrons into account, the resulting levels are broadened and anharmonically shifted. Theory gives us the following relationship (Schönherr et al., 2007) for the Landau energies, starting with the fundamental line according to $n = 1$:

$$E_n = m_e c^2 \frac{\sqrt{1 + 2n(B/B_{\text{crit}}) \sin^2 \theta} - 1}{\sin^2 \theta} \frac{1}{1 + z} \quad (1)$$



Figure 2: INTEGRAL, a picture by ESA

Here m_e is the electron rest mass, c the speed of light and θ the angle between the photon direction and the magnetic field vector. The last term describes the gravitational redshift. There are two possibilities for an excited electron to fall down back in the ground state: it can fall down several levels at once, emitting a photon of energy $n \cdot E_1$. On the other side, it could fall down from one level to the next, each time emitting the ground level energy, E_1 . This process called Photon Spawning can literally fill up the fundamental cyclotron line and leads to emission wings around the fundamental line. Schönherr et al. (2007) and Grämer (2008) provide further explanations on the forming of CRSF and their dependence on diverse parameters.

If the line energies are known, one can estimate the strength of the magnetic field approximately by the “12- B -12 rule”:

$$E_{cyc} \approx \frac{1}{1+z} \cdot 11.57 \text{ keV} \cdot B_{12} \quad (2)$$

where B_{12} denotes the magnetic field in units of 10^{12} Gauss (Schönherr et al., 2007).

4U 0115+63 is the record holding source with respect to the number of detected CRSF: in some spectra one can find up to 5 absorption lines! As Tsygankov et al. (2007), Nakajima et al. (2006) and Heindl et al. (1999) observed already variations of the fundamental line energy with the flux during earlier outbursts, the very interesting question came up how these features behave during the latest outburst in March/April 2008. In this work I will concentrate mainly on this luminosity dependent variations of the fundamental line and its first harmonic as these are the ones visible in most spectra.

2 Data Analysis

2.1 Instruments and Data Reduction

The International Gamma-Ray Astrophysics Laboratory (INTEGRAL) mission was established by the European Space Agency (ESA)¹ for high resolution spectroscopy and imaging of celestial gamma-ray sources in the energy range from 15 keV up to 10 MeV.

¹The INTEGRAL mission on ESA homepage: <http://sci.esa.int/science-e/www/area/index.cfm?fareaid=21>.

On board it has two main instruments, both of them work in the gamma-ray band: the spectrometer SPI (Spectrometer on INTEGRAL) used for energies between 20 keV and 8 MeV and the imager on-board INTEGRAL (IBIS), giving gamma-ray images with a higher angular resolution than any previous instrument.

INTEGRAL also monitors sources in the X-ray (3–35 keV) and optical band using the Joint European X-Ray Monitor (JEM-X) and the optical monitoring camera OMC, respectively (Winkler et al., 2003).

IBIS is an imager optimized for high angular resolution imaging. It uses a coded mask², which is placed 3.2 m above the detection plane. This plane consists of two parallel cameras, PICsIT covering the range from 170 keV to 10 MeV and ISGRI for the low energies between 15 keV up to 1 MeV (I decided to take data between 20–150 keV even less for my fits into account, as in this range they show a good signal-to-noise ratio). For further information, see Lebrun et al. (2003).

On the other hand, JEM-X provides X-ray spectra in the 3 to 35 keV band and images with arcminute angular resolution. Like ISGRI, it also uses the coded-mask technique, but consists of two identical, co-aligned telescopes. Most of the time only one of them is in use. Each of the telescopes has its own mask, one inverted with respect to the other (Lund et al., 2003).

The data from IBIS/ISGRI and JEM-X I analyzed were reduced by Ingo Kreykenbohm. He followed the “OSA-cookbooks” for data reduction, using the default parameters³. Several science windows gathered during one satellite revolution were combined. The six investigated revolutions (later I will just call them spectra denoting them by their revolution number) contain data from 2008, March 21 until April 24.

2.2 Analysis and Modelling

I used a program named ISIS to analyze and model the data. ISIS, the Interactive Spectral Interpretation System, was developed as an interactive tool for studying the physics of X-ray spectrum formation, supporting measurement and identification of spectral features. It provides access to databases of atomic structure parameters and plasma emission models (Houck & Denicola, 2000).

A model named “npex” gave a good fit of the continuum. Mainly it consists of a common power law with exponential cutoff (explained by inverse Comptonization, see Grämer (2008)), slightly corrected by a second power law:

$$\text{NPEX}(E) = N(E^{-\alpha_1} + N_2 E^{-\alpha_2})e^{-E/E_{\text{temp}}} \quad (3)$$

where $N_2 \ll N$, $\alpha_1 > 0$ and $\alpha_2 < 0$.

The iron $K\alpha$ line was modelled with a sharp Gaussian emission line (in ISIS: function “egauss”), but I could not localize it in all spectra. The cyclotron lines could be well described by the function “gabs”, which is an absorption feature of Gaussian shape, too.

But to get really good description of the data, I had to include an additional emission Gaussian located somewhere between 6 and 10 keV in all spectra. This ominous feature (in literature often referred to as the “10 keV Feature”) can be observed in the spectra of many accreting neutron stars but could not satisfactorily be described by now (see Grämer, 2008). I will come back to this strange feature later on.

Note that we are dealing with data sets from two instruments, ISGRI and JEM-X, with different sensitivities. As the two instruments are not really good calibrated with respect to each other, we have to take an additional factor into account which scales one of the two data sets

²For further information on the coded-mask technique see <http://sci.esa.int/science-e/www/object/index.cfm?fobjectid=31175&fbodylongid=724>.

³see a documentation for INTEGRAL data analysis with the OSA 7.0 software on <http://isdc.unige.ch/?Support+documents>

Table 1: Continuum fit parameters.

| no. | N | α_1 | α_2 | E_{temp} | Constant | Time | Flux _{en} | χ_{red}^2 |
|--------|-----------------------|-----------------------|------------|-------------------|----------|---------|-----------------------|-----------------------|
| | keV/s·cm ² | | | keV | | MJD | keV/s·cm ² | |
| 664 | 0.22 | 0.77 | -4.65 | 10.54 | 1.38 | 54546.5 | 5.55 | 1.06 |
| 667 | 0.11 | 4.10·10 ⁻⁸ | -6.30 | 8.28 | 1.37 | 54555.5 | 11.80 | 1.08 |
| 668 | 0.10 | 1.44·10 ⁻⁹ | -7.93 | 8.76 | 1.32 | 54558.5 | 10.12 | 6.36 |
| 669 | 0.33 | 0.51 | -4.87 | 8.75 | 1.37 | 54563.4 | 9.31 | 1.30 |
| 670 | 0.28 | 0.51 | -3.24 | 7.99 | 1.30 | 54566.4 | 7.38 | 1.36 |
| 675 | 0.026 | 8.13·10 ⁻⁹ | -8.31 | 2.72 | 1.40 | 54580.6 | 0.72 | 1.56 |
| bright | 0.14 | 1.79·10 ⁻⁵ | -4.64 | 7.03 | 1.39 | 54546.5 | 7.94 | 1.67 |

relatively to the other. For each of the spectra, we have to fit this scaling constant (here, the ISGRI data set was multiplied by the factor).

As each of the described features contributes its own set of parameters to the fit function, we end up with at least 9 open parameters (just for the continuum!). "Npex" alone has 5 variable parameters, each emission or absorption line adds 3 (line energy, width and depth) and 1 factor scales the data sets. Consider that for a spectrum with three CRSF, we have to find a global minimum (i.e., a set of parameters describing the data best) in a 15-dimensional parameter space!

Figure 3 shows exemplarily the modelling process and the impact of additional features on the continuum. The reader can easily convince herself how the errors become smaller the more lines I included, which is reflected in decreasing χ_{red}^2 .

3 Results

3.1 Continuum

Table 1 shows the best-fit continuum parameters. I also added the 22–90 keV energy flux and the MJD starting time of the measurement. For spectrum bright, the revolutions 664–670 were added.

One can clearly see that the continuum does not remain constant though I could not find obvious correlations between the parameters and the flux.

For some of the spectra (664, 667, 669, 670), I could find well matching models with χ_{red}^2 -values between 1 and 2. This indicates that the model with the distinct set of parameters describes the data counts sufficiently exact. Problems, however, occurred while fitting the lowest flux spectrum 675 (I estimated a 3–50 keV luminosity of $0.65 \cdot 10^{37} \text{ erg s}^{-1}$): the error bars are too large to even find reliable parameters for the continuum or, to be more precisely, one can fit really different models which lead to similar small values for χ_{red}^2 . Figure 4 shows a fit model of the 675 spectrum, but be warned that this set of parameters must not be the only one which yields small χ_{red}^2 ! Nevertheless, I tried at least to find a lower energy limit for the fundamental line by assuming (small) typical values for the line width and depth and including them in the spectrum. I hoped to get a rather great change of χ_{red}^2 . Then I could have excluded a fundamental line at this energy. But unfortunately, the χ^2 changed too slightly to get reliable lower energy limits.

Another problem was the fitting of spectrum 668 (the first revolution after the outburst's peak). It was not possible to find a reasonable set of parameters of the assumed model which would result in small χ_{red}^2 -values. I guess that one has to find different models for describing the source's behavior. But I am afraid I have to postpone the investigation of this characteristics as closer analysis would exceed the given time limits for this work.

So for the further analysis we have to keep in mind that the best-fit models of the four spectra

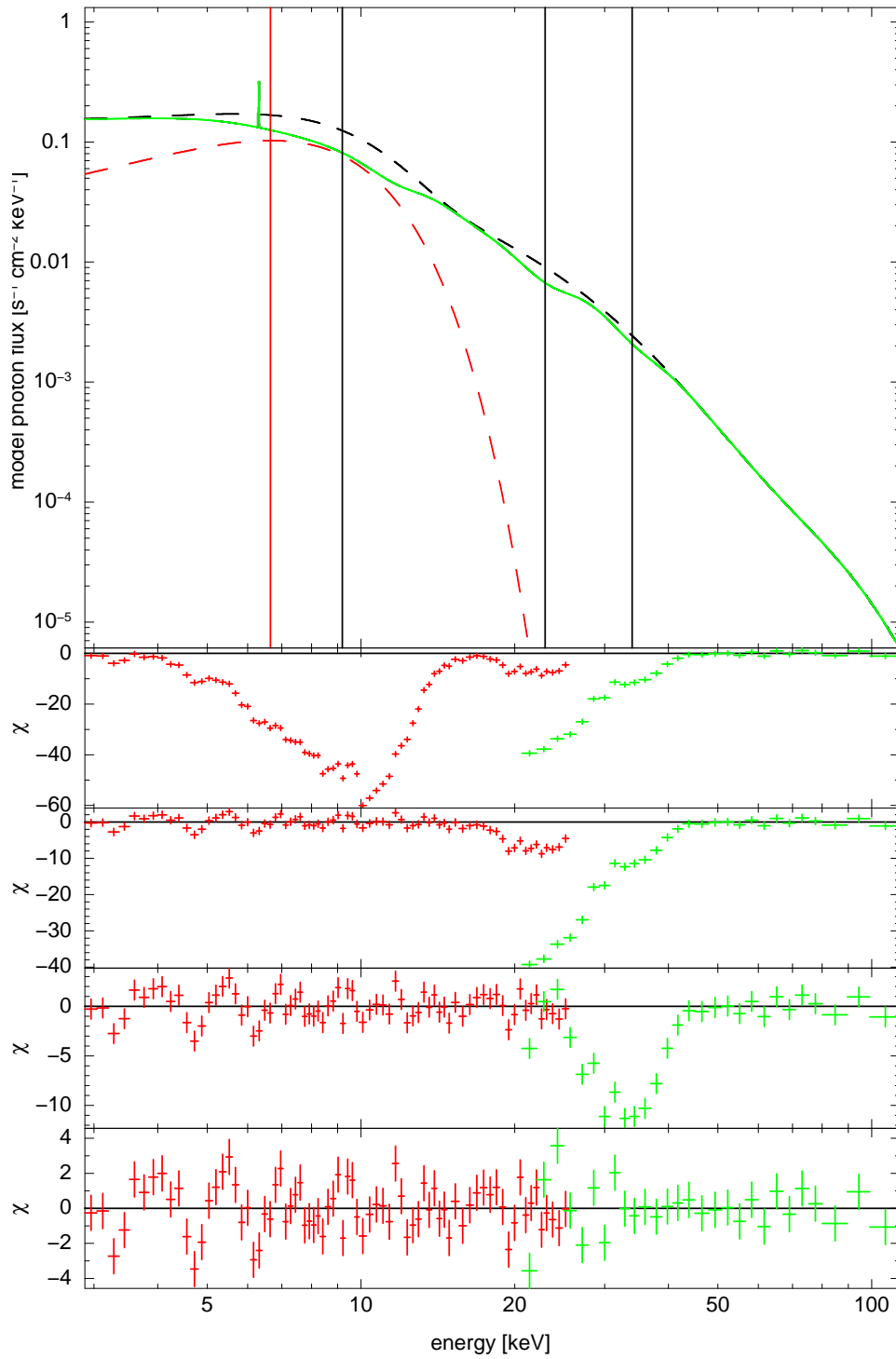


Figure 3: Fit of spectrum 667.

upper panel: The best-fit model (green line) with three CRSF, the “10 keV Feature” alone (dashed red line) and the continuum consisting of “npex”, the “10 keV”-Gaussian and the iron line (dashed black line). The vertical lines denote the position of the CRSF (black) and the Gaussian (red).

panels below: residuals, the first one shows the evaluation of the continuum (“npex”, iron-line and Gaussian) ($\chi_{\text{red}}^2 = 322.4$), the others show top down the model after inclusion of the lines at 9.2 keV ($\chi_{\text{red}}^2 = 28.9$), 22.9 keV ($\chi_{\text{red}}^2 = 4.80$) and 34.0 keV ($\chi_{\text{red}}^2 = 1.08$).

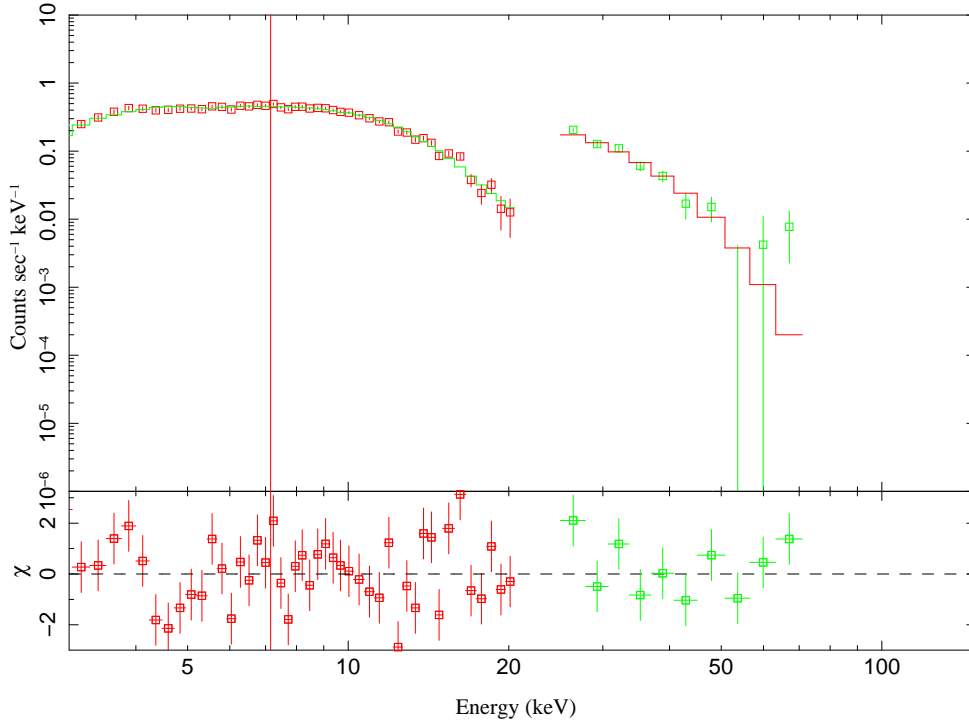


Figure 4: A fit model of the lowest flux spectrum (675) with the Gaussian emission line (red line).

664, 667, 669 and 670 are the most reliable, whereas we have to be careful with information gathered from the other ones.

3.2 Flux Variation during the Outburst

First of all, I want to show how the photon flux of 4U 0115+63 behaves during the observed outburst. The flux is estimated in photons per second and square centimeter by evaluating the best-fit model for each spectrum and integrating it over the energy. It denotes the supposed number of photons arriving at the instrument per second and square centimeter. Note that for the actually detected count rate, this flux is multiplied by the instrument's response matrix and the effective area. These results are compared with data counts from the Burst Alert Telescope (BAT)⁴, an instrument of the Swift Gamma-Ray Burst Mission⁵. For making the values comparable, I estimated the flux values only between 15 and 50 keV and scaled the BAT count rate by a factor of 1.75.

As a pleasant side-effect, we have just discovered a rule of thumb for dealing with BAT count rates: Assuming the evaluated IBIS flux to be the realistic (note that then we have to multiply the factor 1.75 by the data set scaling factor between 1.30 and 1.39), we can estimate the BAT count rate:

$$\frac{\text{BAT count rate}}{\text{counts s}^{-1}\text{cm}^{-2}} \approx 0.41 \cdots 0.44 \cdot \frac{\text{flux}}{\text{photons s}^{-1}\text{cm}^{-2}} \quad (4)$$

i.e., BAT's sensitivity in the given energy range (15–50 keV) lies between 41% and 44%.

⁴The Data are available at <http://swift.gsfc.nasa.gov/docs/swift/results/transients/weak/4U0115p634/>.

⁵For Information on the Swift mission, see <http://swift.gsfc.nasa.gov/>.

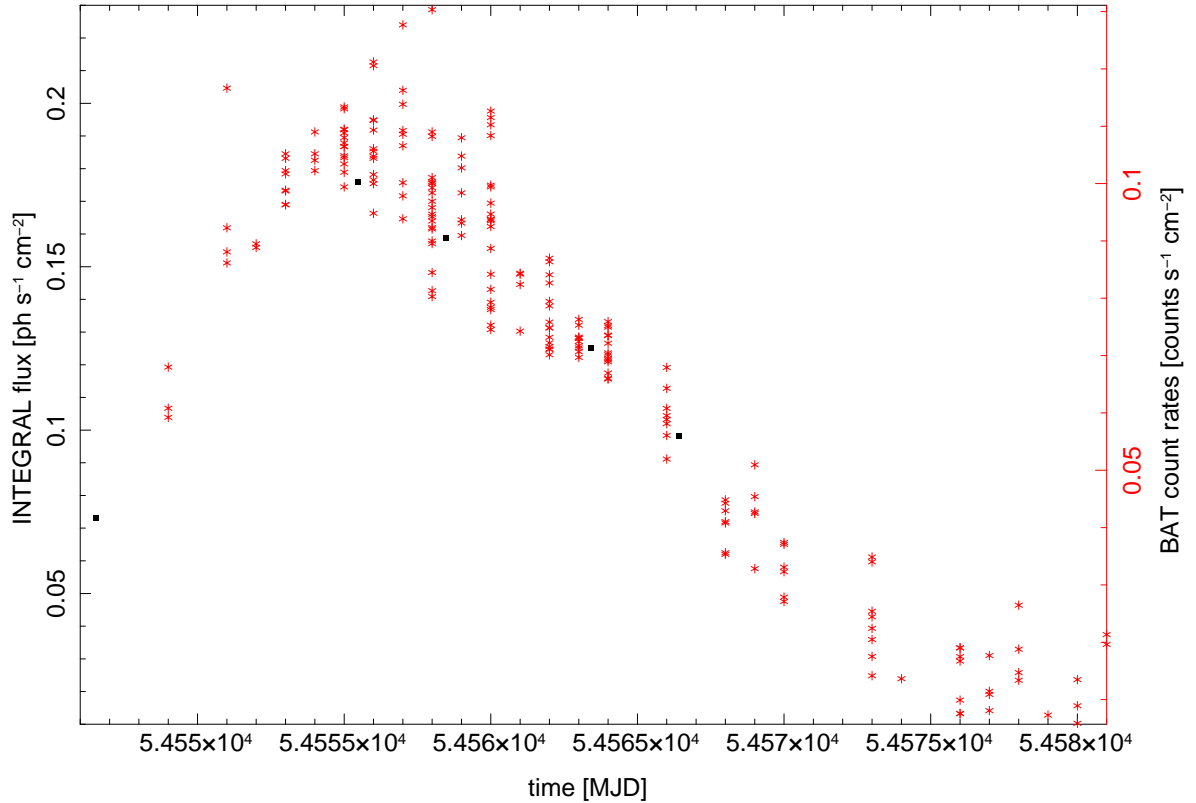


Figure 5: A comparison of the BAT count rates (red crosses) and the estimated flux (black squares) from the INTEGRAL data of the March 2008 outburst (the BAT counts were multiplied by a scaling factor of 1.75).

Figure 5 shows the flux evaluation with the time. One can clearly see the outburst's peak on March 3 (MJD 54555).

3.3 Variation of the CRSF with the Flux

In table 2 I listed all CRSF I could detect in the spectra. The small numbers denote the line energies' confidence intervals. Figure 6 shows all the lines plotted against the luminosity.

As I already mentioned above, the cyclotron line energies have showed flux/luminosity dependence in earlier outbursts (Nakajima et al., 2006). I could also see variations of the CRSF with the luminosity in the March 2008 outburst: Having focused on the fundamental and first harmonic lines, I found that the energy of the first line decreased whereas the second feature remained relatively stable. Of course I wanted to compare my results to the prior data. Therefore I took the 1999 outburst's fundamental line energies and the corresponding luminosities (data from Nakajima et al., 2006, Table 2) and plotted it with my data. Figure 7 shows the result: We see a really good accordance of the values!

Note that for an estimation of the source's luminosity, we need to know the distance to the Earth. Following Nakajima et al. (2006) and Negueruela & Okazaki (2001), I assumed a distance of 7 kpc ($3.0857 \cdot 10^{18}$ cm). Then I calculated the 3–30 keV luminosity by

$$L = 4\pi r^2 f_{\text{en}} \quad (5)$$

where f_{en} is the 3–30 keV energy flux and r denotes the distance to the source.

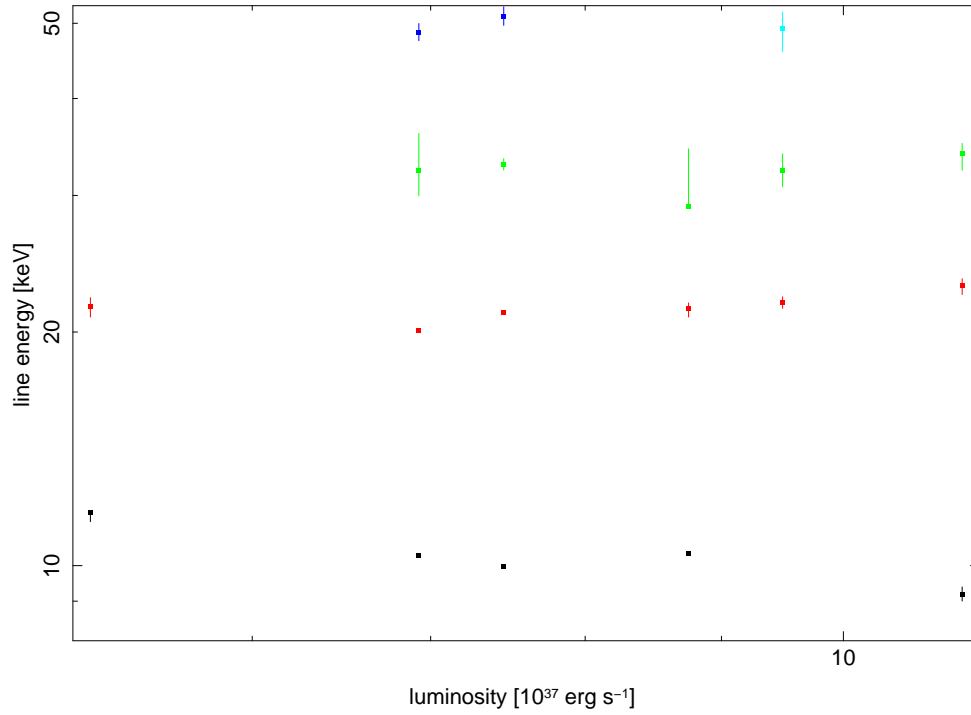


Figure 6: This plot shows all cyclotron features I could identify.

By now, I have not talked about why the CRSF energies vary with the object's luminosity. As I already explained above, the fundamental line energy is related to the B -field strength by

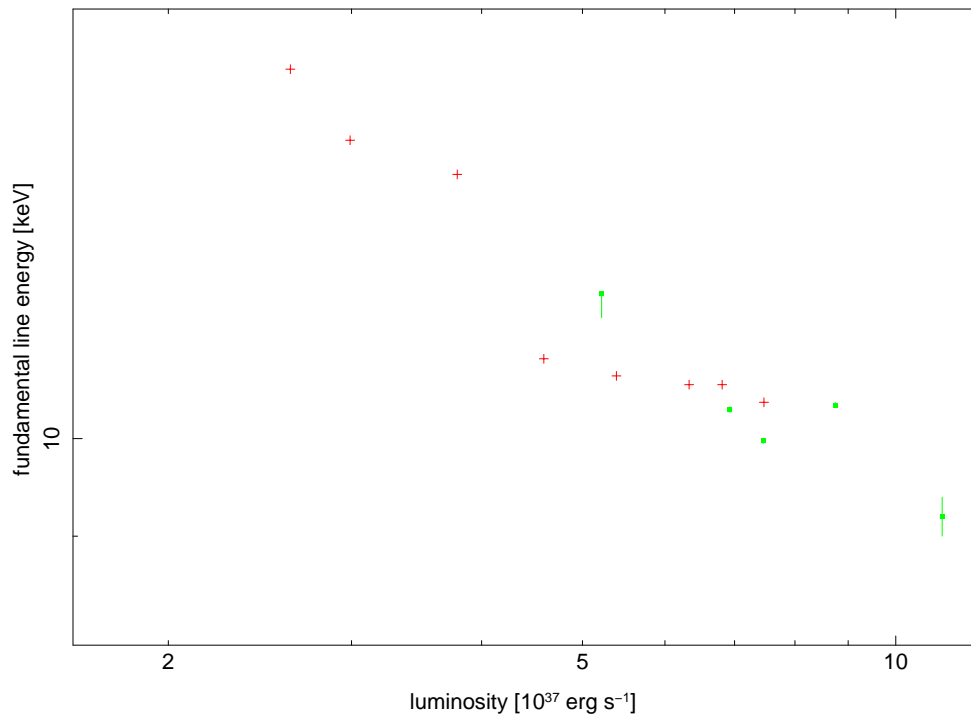


Figure 7: A comparison of the Nakajima data from 1999 (red crosses) and the latest outburst in 2008 (green squares).

Table 2: Line parameters

| no. | E_1 | σ_1 | τ_1 | E_2 | σ_2 | τ_2 |
|--------|------------------------|------------|----------|-------------------------|------------|----------|
| | keV | keV | | keV | keV | |
| 664 | $11.7^{+0.0}_{-0.3}$ | 1.25 | 0.61 | 21.6 ± 0.6 | 1.33 | 0.46 |
| 667 | $9.19^{+0.20}_{-0.19}$ | 1.99 | 11.73 | $22.9^{+0.5}_{-0.6}$ | 2.78 | 2.08 |
| 668 | 0 | 0 | 0 | 21.8 ± 0.4 | 2.99 | 3.05 |
| 669 | 10.37 ± 0.03 | 1.24 | 7.33 | $21.4^{+0.4}_{-0.5}$ | 2.80 | 1.28 |
| 670 | 10.32 ± 0.03 | 1.31 | 6.30 | $20.07^{+0.04}_{-0.09}$ | 0.04 | 14.99 |
| bright | 9.97 ± 0.03 | 1.44 | 3.63 | $21.17^{+0.14}_{-0.09}$ | 4.96 | 5.61 |
| no. | E_3 | σ_3 | τ_3 | E_4 | σ_4 | τ_4 |
| | keV | keV | | keV | keV | |
| 664 | 0 | 0 | 0 | 0 | 0 | 0 |
| 667 | $34.0^{+1.1}_{-1.6}$ | 3.8 | 1.52 | 0 | 0 | 0 |
| 668 | $32.3^{+1.7}_{-1.5}$ | 5.58 | 5.69 | 49 ± 3 | 7.81 | 6.31 |
| 669 | 29^{+5}_{-0} | 8.83 | 3.62 | 0 | 0 | 0 |
| 670 | 32^{+4}_{-2} | 2.13 | 0.269 | $48.7^{+1.3}_{-1.2}$ | 12.74 | 6.40 |
| bright | $32.9^{+0.6}_{-0.5}$ | 2.60 | 0.95 | $51.0^{+1.5}_{-1.3}$ | 17.25 | 16.48 |

the 12- B -12 rule, Equation (2). So does the magnetic field of a neutron star really change while accreting matter from its companion? No, indeed. But what is supposed to vary is the height of the accretion column: With decreasing luminosity, the radiative pressure in the column becomes smaller and therefore the line forming region sinks down towards the neutron star’s surface. And as the B -field should be stronger the closer one gets to the surface, one expects to observe decreasing line energies (Nakajima et al., 2006).

3.4 Estimation of the Magnetic Field Strength

Having identified the CRSF positions, we can now calculate the B -field of 4U 0115+63. According to the 12- B -12 rule (2), it is given by

$$B_{12} \approx (1+z) \cdot \frac{E_{\text{cyc}}}{11.57 \text{ keV}} \quad (6)$$

For the estimation, it is reasonable to take the highest identified fundamental cyclotron line (which is formed closest to the star’s surface), $E_{\text{cyc}} = 11.7^{+0.0}_{-0.3}$ keV. Furthermore I assume a gravitational redshift of $z = 0.3$ according to Grämer (2008). We therefore obtain a magnetic field of $B_{\text{estim}} = 1.31^{+0.0}_{-0.03} \cdot 10^{12}$ G.

3.5 The “10 keV Feature”

In many neutron stars’ spectra, one observes a remarkable feature in the energy range between 8 keV and 13 keV. This so-called “10 keV feature” is a Gaussian-shaped broad peak. It could not be explained by now but it seems to be related to the stars’ magnetization (Grämer, 2008).

The spectra I examined also showed this characteristic peak (Note that in my fits, the feature sometimes appears at even lower energies than 8 keV). I tried several models (some of them more physical reasonable than others): Blackbody radiation, bremsstrahlung, partial covering and a blackbody disk – none of these could describe the data sufficiently exact.

Having failed in these attempts, I tried something different: Taking only the four “reliable” spectra into account, I plotted the location of the fundamental lines and of the Gaussian feature

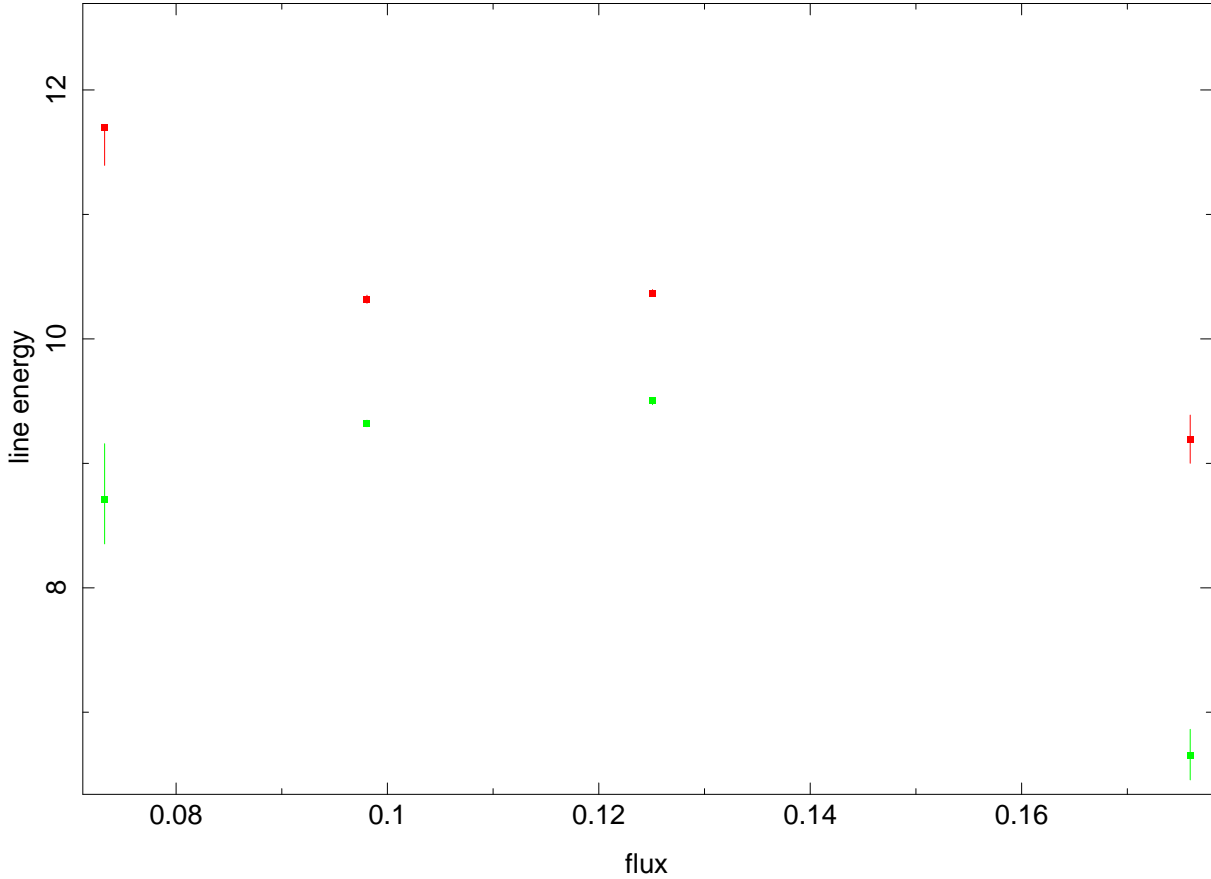


Figure 8: The fundamental line energies (red) and the Gaussian feature (green).

Table 3: Best-fit parameters of the Gaussian.

| no. | E_{Gauss} | σ_{Gauss} | $area_{Gauss}$ |
|--------|------------------------|------------------|----------------------|
| | keV | keV | ph/s·cm ² |
| 664 | $8.7^{+0.5}_{-0.4}$ | 3.48 | 0.13 |
| 667 | 6.6 ± 0.2 | 3.32 | 0.63 |
| 668 | 6.39 ± 0.05 | 2.31 | 0.20 |
| 669 | $9.50^{+0.02}_{-0.03}$ | 1.94 | 0.20 |
| 670 | 9.32 ± 0.03 | 2.18 | 0.19 |
| 675 | $7.2^{+0.2}_{-0.4}$ | 4.44 | 0.04 |
| bright | 9.29 ± 0.02 | 1.74 | 0.11 |

against the luminosity (figure 8). I think one can clearly see that the Gaussian is somehow related to the fundamental line energy as its position decreases similarly and therefore I suppose that it is nothing else than just the very large emission wing of the first cyclotron line.

4 Summary

I have obtained several results during my work about the March 2008 outburst of 4U 0115+63.

Having evaluated the flux during the outburst, I intended to compare it with count rates gained from BAT observations of the same time. As I had to scale the count rates with respect to the flux, I found a rough estimation of BAT's sensitivity in the energy range of 15 to 50 keV:

It detects about 41% to 44% of the incoming photons.

Furthermore (and this was the primary intention of this work), I could detect a cyclotron line and up to three harmonics. In former data, the fundamental line energy was shown to be flux dependent which I could approve in the latest outburst's spectra. A comparison with the March/April 1999 data (Nakajima et al., 2006) revealed a similar relation of the CRSF position with the luminosity.

Knowing the highest fundamental line position, the neutron star's magnetic field strength could be estimated. The 12-*B*-12 rule revealed a value of $B_{\text{estim}} = 1.31_{-0.03}^{+0.0} \cdot 10^{12}$ G, which is consistent with former calculations. Grämer (2008) and Tsygankov et al. (2007) obtained values of $1.3 \cdot 10^{12}$ G and $1.4 \cdot 10^{12}$ G, respectively.

Searching for an explication of the “10 keV feature”, I found its energy to be related to the first CRSF position. This fact suggests that the feature is actually just the very pronounced emission wing of the fundamental line.

I am afraid that I could not investigate all of the source's characteristics, so some open questions do still remain: I am sure it would be interesting to study the dependency of the continuum model on different parameters like the time, the luminosity or the line energies. The most challenging and promising task would be to find another model describing the 668 spectrum. In my opinion, one could learn a lot about 4U 0115+63 if the unordinary behavior shortly after the outburst's peak could be explained.

References

- Grämer C., 2008, Zyklotronlinien – eine RXTE-Sample, Zulassungsarbeit an der Dr. Reimeis-Sternwarte Bamberg
- Heindl W.A., Coburn W., Gruber D.E., et al., 1999, *apjl* 521, L49
- Houck J.C., Denicola L.A., 2000, In: Manset N., Veillet C., Crabtree D. (eds.) *Astronomical Data Analysis Software and Systems IX*, Vol. 216. Astronomical Society of the Pacific Conference Series, p.591
- Lebrun F., Leray J.P., Lavocat P., et al., 2003, *aap* 411, L141
- Lund N., Budtz-Jørgensen C., Westergaard N.J., et al., 2003, *aap* 411, L231
- Nakajima M., Mihara T., Makishima K., Niko H., 2006, *apj* 646, 1125
- Negueruela I., Okazaki A.T., 2001, *aap* 369, 108
- Schönherr G., Wilms J., Kretschmar P., et al., 2007, *aap* 472, 353
- Tsygankov S.S., Lutovinov A.A., Churazov E.M., Sunyaev R.A., 2007, *Astronomy Letters* 33, 368
- Winkler C., Courvoisier T.J.L., Di Cocco G., et al., 2003, *aap* 411, L1

List of Figures

| | | |
|---|---|----|
| 1 | Neutron star X-ray binary | 3 |
| 2 | INTEGRAL | 4 |
| 3 | Fit of spectrum 667 | 7 |
| 4 | Fit of spectrum 675 | 8 |
| 5 | BAT and INTEGRAL | 9 |
| 6 | All cyclotron lines | 10 |
| 7 | Nakajima and INTEGRAL | 10 |
| 8 | Fundamental CRSF and “10 keV feature” | 12 |

List of Tables

| | | |
|---|--|----|
| 1 | Continuum fit parameters. | 6 |
| 2 | Line parameters | 11 |
| 3 | Best-fit parameters of the Gaussian. | 12 |